Eur Biophys J (1987) 15: 27–33

European Biophysics Journal

A comparison of sodium channel kinetics in the squid axon, the frog node and the frog node with BTX using the "silent gate" model

D. T. Edmonds

The Clarendon Laboratory, Parks Road, Oxford OX1 3PU, United Kingdom

Received November 25, 1986/Accepted in revised form March 17, 1987

Abstract. In this paper it is shown that the very different kinetics measured for the rise of the sodium current which follows a depolarization of the membrane in the squid giant axon, the frog node and the frog node treated with Batrachotoxin may be accurately predicted using only the measured equilibrium and static characteristics for the three preparations and the kinetics measured for the gating charge transfer.

The kinetic predictions follow the use of the "silent gate" model for ion channel gating. The model is electrostatic and its chief assumptions are that the channel gate, called here the N-system, has fast kinetics and responds to the gating charge that transfers but not directly to the trans-membrane voltage applied. Because channel gating, corresponding here to the motion of the N-system, does not change its energy in the *trans*-membrane applied electric field the gating is electrically silent as far as gating charge transfer measurement is concerned. However the probability of gating rises with the quantity of gating charge that transfers due to the electrostatic interaction between the N-system and the gating charge, redistributed under the influence of the applied *trans*-membrane electric field. With these assumptions the kinetics of sodium channel gating are predictable using only the static and equilibrium characteristics of gating charge and channel activation measured as a function of membrane voltage, and the kinetics of the gating charge transfer. Because of the fast kinetics assumed for the N-system the predicted kinetics are the same for channels with any number of equivalent and independent N-systems or gates acting in parallel.

The model predictions for sodium permeability kinetics are compared in detail with those recently measured for the frog node treated with Batrachotoxin and excellent agreement is obtained.

Key words: Model ion channel, sodium channel

Introduction

The kinetic properties of the membrane spanning sodium channel in excitable tissue are known to be very different when measured in the squid giant axon, the frog node of Ranvier and the Batrachotoxin (BTX) modified frog node. For the squid axon the sodium current increase, following a suitable depolarizing excursion of the membrane voltage, is notably sigmoid in character and follows approximately the predictions of the Hodgkin and Huxley (1952) m^3 model. For the frog node the current increase is less sigmoid and is often fitted by a Hodgkin and Huxley model using m^2 rather than m^3. The BTX modified frog node displays a sodium current increase which is almost a simple exponential with little sigmoid character.

In this paper a comparison of the equilibrium and kinetic characteristics of the sodium channel in these three preparations is made using the "silent gate" model described previously (Edmonds 1985, 1987) to show that the very different kinetic behaviour displayed in the three cases is predictable by their different static equilibrium characteristics.

Experimental

The two chief equilibrium characteristics measured when the sodium channel is studied experimentally are the sodium permeability and the gating charge transfer measured as a function of the voltage $VM = V_{in} - V_{out}$ applied across the membrane. A recent review of such measurements in the squid axon has been provided by Keynes (1983). Figure 1 a shows as circles the gating charge transfer and as squares the change in sodium conductance for the squid axon plotted against the membrane voltage VM in mV. The data were kindly provided by Prof. R. D. Keynes. It is known that the instantaneous I

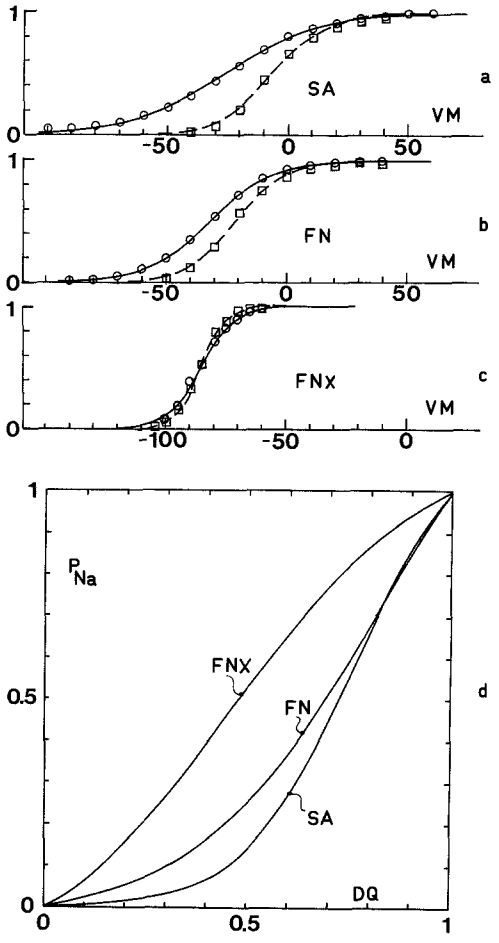

Fig. 1. a – c refer respectively to the squid axon (*SA*), the frog node (*FN*) and the frog node when treated with Batrachotoxin (*FNX*). The circles in each case give the experimentally measured equilibrium gating charge transfer, normalized to unity and measured as a function of the applied membrane voltage *VM* in mV. The squares give the membrane voltage dependent change in the sodium channel permeability plotted in the same manner. The sources of the experimental data are given in the text. The continuous lines through the circles and squares are the best fit of Eq. (1) to the equilibrium gating charge transfer resulting in the determination of the constants *ZQ* and *VQ* and of Eqs. (2) and (3) to the equilibrium sodium permeability leading to the determination of the constants *VN* and *VNQ*. **d** Shows a direct plot of the normalized change in sodium permeability DP_{Na} against the normalized gating charge transfer *DQ* predicted by the model with its four parameters determined as above for the squid axon (*SA*), the frog node (*FN*) and the frog node treated with BTX (*FNX*). In the model, the value of *DQ* normalized to unity as in this figure, is denoted by *q*

vs. *V* curve for the squid axon is non-linear at membrane voltages more negative than −50 mV (Stimers et al. 1985), but at the membrane voltages of interest here of −40 mV to +40 mV it is linear so that I will assume that the change in the conductance measured represents a change in the average number of channels open. In Fig. 1 b are plotted the gating charge transfer and the sodium permeability change for the frog node. The gating charge transfer in this case is plotted as circles using the analytical expression quoted by Dubois and Schneider (1982). The sodium permeability data, shown as squares, was sent to me by Prof. H. Meves. In this case, due to the marked curvature of the instantaneous *I* vs. *V* characteristic for the frog node, the conductance change must be corrected if it is to reflect the probability of channel opening (Dodge and Frankenhauser 1959). The permeability data displayed here have been so corrected as described by Bergman and Meves (1981) and shown by these authors as their Fig. 15. The data for the BTX modified frog node displayed as circles and squares in Fig. 1 c was sent to me by Prof. J. M. Dubois and was displayed in Dubois et al. (1983). I am most grateful to Profs. Dubois, Keynes and Meves who so freely sent me their numerical data.

The differences between the measured equilibrium characteristics of the sodium channel in the three preparations is clear in Fig. 1 a – c. Most striking is the difference in the positions of the gating charge transfer characteristic relative to that for the sodium permeability change and the differences in the shapes and maximum slopes of the various curves.

The silent gate model

The model was first described (Edmonds 1983) as a much simplified system with only four states in which a single gating particle with only two states represented the measured gating charge transfer. Subsequently the model has been refined so that the gating charge transfer is assumed to occur continuously, representing the cumulative effects of many microscopic dipole reversals or charge movements in the vicinity of the channel. In a previous paper (Edmonds 1987) I have described the experimental evidence that directly supports a model of this type, and given examples of real physical systems that it could represent. I have also attempted to show by highly simplified but quantitative calculations that one realization of the model using the known large electric dipole moment of the alpha-helix is physically realistic (Edmonds 1985), so that here I will only describe the essentials of the model, referring to one possible realization shown in Fig. 2, before discussing its predictions for the three sodium channel preparations.

The model has two components called the *Q* and the *N*-systems. The *Q*-system represents the electrical response of the channel to the voltage *VM* applied across the membrane and could include the

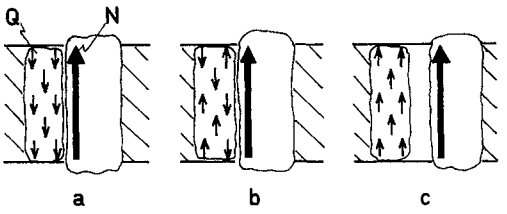

Fig. 2 a – c. A sketch of three states of one possible realization of the model. The Q-system is represented by a polarizable cylinder spanning the membrane and the N-system is represented by a closely neighbouring alpha-helix with its electric dipole moment pointing outward. In **a** the membrane is in its resting configuration with the inside negative relative to its outside and the Q-system consequently polarized in an inward direction. In this configuration the Q and N-systems attract each other electrostatically leading to a closed channel. In **c** is shown the final state arrived at after a large depolarizing pulse has been applied to the membrane such that its inside is now positive and the Q-system has reversed its electric dipole moment to be pointing outward. The Q and N-systems now repel each other leading to the sideways translation of the N-system and the opening of a *trans*-membrane ion channel. In **b** is shown an intermediate state in which some of the dipole moment of the Q-system has reversed but has not reached the threshold required to ensure channel opening

motion of mobile charged groups and the rotation of electric dipoles such as water molecules. In Fig. 2 it is represented by a polarizable cylinder spanning the membrane. The displacement current that results from the charge transfer is measured as gating charge transfer. The membrane voltage dependent charge transfer in the Q-system is represented by the continuous variable q so that $q=0$ represents the state with the inside of the membrane very negative and $q=1$ represents the saturated transfer that occurs for very positive *trans*-membrane voltages differences.

The measured gating charge transfer shown in Fig. 1 a – c can be well represented by expressions of the form

$$q(VM) = 1/\{1+\exp[-ZQ(VM-VQ)/VT]\}, \quad (1)$$

where $VT = KT/|e| = 25\,\text{mV}$ with K the Boltzmann constant, T the absolute temperature and $|e|$ the proton charge. The constants ZQ and VQ give the "effective valence" of the transferred charge and the membrane voltage in mV for which $q(VM)=0.5$. The continuous lines through the circles in Fig. 1 a – c show the best fit of the experimental data to Eq. (1) leading to values of the pair of constants ZQ and VQ of 1.33 and -25 mV, 1.93 and -32 mV and 3.82 and -85.6 mV respectively.

The N-system represents the gating mechanism of the channel and for simplicity it will be assumed to have only two states, shut represented by $n=0$ and open represented by $n=1$. The N-system does not change its electrostatic energy in the *trans*-membrane electric field when it makes its transition and is thus electrically silent as far as the measurement of gating charge transfer is concerned. The N-system transition is represented in Fig. 2 as the sideways translation of an alpha-helix in the close vicinity of the channel. Because such a sideways transition does not change the electrostatic energy of the N-system in the *trans*-membrane electric field the N-system can not move as a direct response to a change in the *trans*-membrane field. The N-system does however interact electrostatically with the Q-system in that the probability of the N-system making a transition from $n=0$ to $n=1$ increases as q increases.

The silent gate model is thus seen to be a threshold model which will open or shut when the gating charge transferred approaches some critical value. Such an assembly may be represented by writing the excess energy of the state $n=1$ over the state $n=0$ as $DU(q)$ in

$$DU(q) = |e| \cdot (VN - q \cdot VNQ),$$

so that

$$DU(q=0) = |e| \cdot VN$$

and

$$DU(q=1) = |e| \cdot (VN - VNQ).$$

Here VN and VNQ are parameters expressed in mV which characterize the energy state of the N-system in its two configurations. In Fig. 2 the energy difference $DU(q)$ represents the increasing energy of repulsion between the outward pointing electric dipole moment of the alpha-helix and the increasingly outward pointing dipole moment of the polarizable cylinder. The normalized probability that the N-system is in the state represented by $n=1$ due to the change in q is given by $P(n=1)$ in

$$P(n=1) \quad (2)$$
$$= [N(q) - N(q=0)]/[N(q=1) - N(q=0)],$$

where

$$N(q) = 1/\{1+\exp[DU(q)/KT]\}$$
$$= 1/\{1+\exp[(VN - q \cdot VNQ)/VT]\}. \quad (3)$$

The full line through the squares in Fig. 1 a – c is the best fit of Eq. (2) to the experimental data for the sodium channel permeability in the three cases. The model is seen to reproduce the shape of the experimental curves well and the values of the pairs of parameters VN and VNQ so obtained are 145.4 mV and 192.4 mV, 91.84 mV and 111.56 mV and 49.85 mV and 106.9 mV respectively. In the case of the frog node with BTX the model does predict a value of channel permeability change that crosses

the gating charge transfer curve and saturates first as found experimentally. Such a feature is not possible in series sequential models. Of particular interest is that the value of VNQ is almost the same for the frog node with and without BTX while there is a marked change in VN, so that the effect of BTX on the sodium channel permeability may be simply characterized in this model as a change in the energy difference between the two states of the N-system as measured by the change in one parameter VN.

A graphic method of contrasting the differences of the equilibrium characteristics of the sodium channel in the three preparations is shown in Fig. 1 d in which $P(n=1)$ is plotted directly against q using the parameters that fit the experimental data.

Kinetic predictions of the model compared with experiment

I turn now to the kinetic predictions of the model. The only assumption incorporated in the model in this regard is that the transition of the N-system is very fast in comparison with the charge transfer in the Q-system so that the N-system is always in equilibrium with the instantaneous value of q determined by the Q charge transfer. Thus Eqs. (2) and (3) are always true and the kinetic variation of $P(n=1)$ is determined entirely by the time variation of $q(t)$, discussed below, together with the static relationship of $P(n=1)$ to q as represented in Fig. 1 d.

To illustrate the kinetic features of the model we will for simplicity assume that the time variation of q is given by

$$q(t) = q_i + (q_f - q_i) \cdot (1 - \exp(-t/TQ)), \quad (4)$$

where q_i and q_f are the initial and final values of the total normalized gating charge transfer and

$$TQ = 2 \cdot T_{max} / \{\exp[ZQ \cdot (VM - VQ) \cdot f/VT] + \exp[-ZQ \cdot (VM - VQ) \cdot (1-f)/VT]\}, \quad (5)$$

where T_{max} is the maximum value of the relaxation time TQ which occurs at a membrane voltage $VM = VQ$ and f is a constant $0 < f < 1$. Equations (1), (4) and (5) represent what is expected (Adrian 1978) if a number of non-interacting charges of valence ZQ move between two states with energies

$$EQ(0) = ZQ \cdot (VM - VQ) \cdot f \quad \text{and}$$

$$EQ(1) = -ZQ \cdot (VM - VQ) \cdot (1-f)$$

over a barrier of height B such that

$$2 \cdot T_{max} = 1/[R \cdot \exp(-B/KT)],$$

where R is the universal rate constant. This is an accurate description of experimental observations for the frog node (Meves and Rubly 1986) and for the frog node treated with BTX (Dubois and Schneider 1985). It is only an approximation for the squid axon where the gating charge is known to be heterogeneous with at least two components (Khodorov 1979; Peganov 1979; Greef et al. 1982).

The experimental data for the kinetics of sodium channel permeability are usually expressed in terms of the Hodgkin and Huxley (1952) model with the change of a parameter m with time represented by $m(t)$ in

$$m(t) = m_i + (m_f - m_i) \cdot \{1 - \exp[-(t-d)/TM]\},$$

where m_i and m_f are the initial and final values of m and TM is a relaxation time. The change of the sodium channel permeability is then represented by DP_{Na} in

$$DP_{Na} = m(t)^X. \quad (6)$$

In order to fit the Hodgkin and Huxley model to the experimental data it has been found necessary to introduce the time delay d often called the Cole and Moore delay after the investigators who first observed the effect for the potassium channel (Cole and Moore 1960).

For the squid axon, Keynes and Kimura (1983) found that the sodium channel kinetics were well represented by an equation such as (6) with a value of X between 2.9 and 4.4. Figure 3 a and b show a comparison of the predictions of the silent gate model, with its 4 parameters ZQ, VQ, VN and VNQ determined above from the static characteristics, shown as the full line and the predictions of a Hodgkin and Huxley model with delay and a fixed value of $X=3$ shown as circles. It can be seen that the sigmoid behaviour that is found experimentally and is represented here by the Hodgkin and Huxley model predictions is indeed accurately reproduced by the present model. Further examples of such agreement for the squid axon including a comparison of the delay d required to fit the model on the one hand and the experimental data on the other is given in Edmonds (1987). In all the predictions shown in Fig. 3, T_{max} is taken as 1 in Eq. (5) and all the predicted relaxation times and delays will scale with this number.

Although not shown here, the deactivation kinetics of the squid axon, experimentally measured by Keynes and Kimura (1983), are equally accurately predicted (Edmonds 1987) by the model Eqs. (2) and (3) using the time variation of $q(t)$ predicted by Eqs. (4) and (5). The deactivation kinetics are close to simple exponential decays and are not markedly sigmoid essentially because the critical

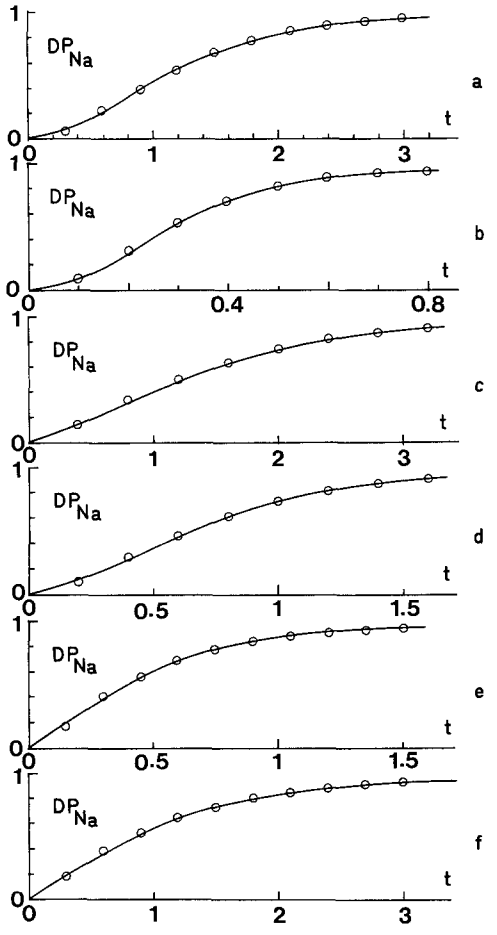

Fig. 3 a – f. In **a** and **b** are displayed as full lines the kinetic predictions of the model for the squid axon, represented by Eqs. (3) and (2) using the time variation of $q(t)$ given by Eqs. (4) and (5) with $f = 1/2$. The four parameters of the model ZQ, VQ, VN and VNQ are determined by fitting Eqs. (1) and (2) to the static characteristics of the squid axon displayed in Fig. 1 a. The times are scaled such that $T_{max} = 1$ in Eq. (5). In **a** and **b** are displayed the model predictions for the change of sodium permeability resultant upon a sudden excursion of the applied membrane voltage from a resting value of -50 mV to values of 0 and $+50$ mV respectively. The circles are the predictions of a Hodgkin and Huxley m^3 model with delay as described by Eq. (6). The pairs of values of TM and d required by the m^3 model are 0.764 and 0.125 and 0.191 and 0.040 respectively. All the values of TM and **d** quoted here again scale with the value of 1 assumed for T_{max} in Eq. (5). In **c** and **d** are shown similar comparisons of the model predictions for the frog node with an m^2 model with delay assuming a resting membrane voltage of -100 mV and membrane voltage excursions to -30 mV and 0 mV respectively. The values for the pair of parameters TM and d required by the m^2 model are 1.10 and 0.133 and 0.52 and 0.095 respectively. In **e** and **f** is shown a comparison between the model prediction and an m^1 model with delay for the frog node treated with BTX assuming a resting membrane voltage of -120 mV and membrane voltage excursions to -70 and -90 mV. The values of TM and d required by the m^1 model were 0.452 and 0.066 and 1.061 and 0.085, respectively

value of q that leads to channel gating is much closer to 1 than to 0.

For the frog node it has been shown that the experimentally determined sodium channel kinetics can be well represented by a m^2 model with delay (Meves and Rubly 1986). In Fig. 3 c and d are shown as full lines the predictions of the model with its parameters fully determined by the static characteristics for the frog node compared with a Hodgkin and Huxley model with delay and $X = 2$. Here the model reproduces the less sigmoid nature of the sodium permeability characteristic for the frog node with equal accuracy.

For the frog node treated with BTX the sodium channel kinetics can to good accuracy be treated as a simple exponential, equivalent to a m^1 model with delay, provided that the earliest part of the sodium current increase is not included (Dubois and Schneider 1985). In Fig. 3 e and f are displayed the model predictions as a full line and the predictions of a m^1 model with delay as circles. With the possible exception of the early points the agreement is again excellent.

The paper by Dubois and Schneider (1985) shows that the gating charge transfer in the BTX treated frog node is simply exponential and gives details of the relaxation behaviour of both the gating charge transfer and sodium permeability measured under the same conditions. It is thus possible to make a more detailed comparison between the model predictions and experiment than is contained in Fig. 3. The experimental curve showing the gating charge relaxation time TQ against VM the membrane voltage is asymmetric about its peak but can be fitted by Eq. (5) with the values of ZQ and VQ determined previously, together with values of $T_{max} = 1.41$ ms and $f = 0.65$. To describe their experimental data on sodium conductance kinetics, Dubois and Schneider used equations of the form

$$I_{Na}(t) = I_{Na}(\infty) \cdot \{1 - \exp[-(t-d)/T_{Na}]\}, \qquad (7)$$

and determined the relaxation time T_{Na} and the delay d as a function of membrane voltage VM. Equation (7) is not the same as the m^1 model used in Fig. 3 e and f unless m_i is always taken as zero but was used simply as a convenient empirical formula that is capable of reproducing the experimental data except at the smallest values of t.

As a sensitive test of the model applied to the frog node treated with BTX, predictions of the model were treated by the procedures of Dubois and Schneider exactly as if they were experimentally generated data. In this manner the parameters TQ and T_{Na} used in the interpretation of the experimental data can be generated by the model so that a direct comparison of the ratios TQ/T_{Na} predicted by

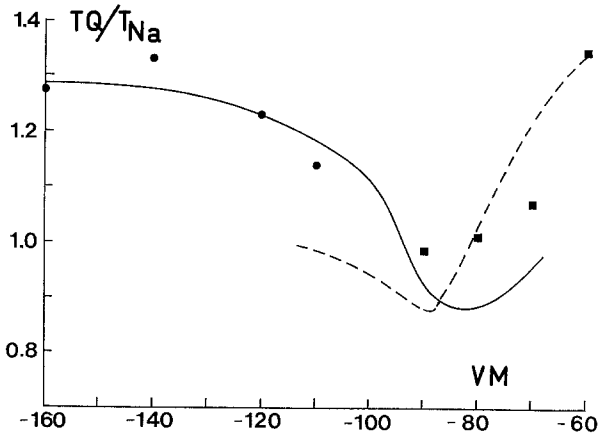

Fig. 4. The filled circles and squares give the ratio of TQ/T_{Na} measured by Dubois and Schneider (1985) in the frog node with BTX, for various sudden excursions of the membrane voltage from initial values of -60 mV and -120 mV respectively. The gating charge transfer relaxation time TQ was found to fit an equation identical to Eq. (4) with TQ given by Eq. (5) with $T_{max} = 1.41$ ms and $f = 0.65$. T_{Na} was obtained by fitting the experimental kinetics of sodium channel conductance to Eq. (7). To compare the predictions of the silent gate model with the experiments on the frog node with BTX, the model predictions were treated as experimental data in exactly the manner described above to generate TQ and T_{Na} and thus the ratio TQ/T_{Na}. The full curve relates to membrane voltage excursions from an initial value of -60 mV and the broken curve from an initial value of -120 mV. The static model parameters ZQ, VQ, VN and VNQ were determined by fitting Eqs. (1), (2) and (3) to the experimental data in Fig. 1 c as described in the text. The kinetics assumed for $q(t)$ were those predicted by Eqs. (4) and (5) with $T_{max} = 1.41$ ms and $f = 0.65$ as found experimentally

the model can be made with those generated by experiment under identical conditions. The model parameters ZQ, VQ, VN and VNQ used for the generation of model data were those leading to the static characteristics shown in Fig. 1 c. The values of $q(t)$ were those generated by Eq. (4) with TQ given by Eq. (5) with $T_{max} = 1.41$ ms and $f = 0.65$ as found experimentally.

In Fig. 4 is shown the model predicted ratio of TQ/T_{Na} following sudden excursions of the membrane voltages VM starting from a resting membrane voltage of -60 mV (full line) and -120 mV (broken line). The values of the ratio obtained by Dubois and Schneider are shown as filled circles when starting from -60 mV and filled squares when starting from -120 mV. The experimental data for T_{Na} and TQ used are those displayed in Dubois and Schneider (1985) as Fig. 5 and kindly supplied to me in numerical form by Prof. Dubois.

The agreement is seen to be remarkedly good, particularly as the connection between the sodium permeability kinetics and the gating kinetics are totally detemined by the two parameters VN and VNQ in Eqs. (2) and (3) which are in turn fixed by the static equilibrium permeability characteristic.

Conclusions

The strongest prediction of the silent gate model is that the gating kinetics of a voltage gated membrane channel are determined solely by the kinetics of the gating charge transfer together with the shapes of the two static characteristics displayed in Fig. 1 a – c. The relationships between these static characteristics are compactly displayed in Fig. 1 d. The shapes shown in this figure are the same statically or dynamically due to the fast response assumed for the N-system. After an excursion of the membrane voltage the kinetics of the gating charge transfer determine a time dependent excursion along the q axis of Fig. 1 d from q_i to q_f. The predicted time dependent excursion along the P_{Na} axis is obtained by reflecting the q excursion in the curve appropriate for the particular preparation being studied. This predicts the kinetics of the channel gating that will result from the original membrane voltage excursion. That the predictions appear to be true for the very different kinetics of the sodium channel in the three preparations described here can be seen in Fig. 3. The differences in the shapes predicted for the three preparations is particularly apparent when a comparison is made between Fig. 3 a, c and f for which the time scales are the same.

Another less obvious consequence of the assumption of fast response for the N-systems is that the model predicts the same kinetics for a channel with a multiple N-system. Let us assume for instance that the channel has two identical N-systems, possibly alpha-helices as in Fig. 2, which act independently. Then the probability of the channel being open will be given by the square of $P(n=1)$ in Eq. (2) so that it is now necessary to fit the square of $P(n=1)$ to the experimental values of P_{Na}, resulting in altered values of VN and VNQ. However the form of Fig. 1 d is unchanged and so are the sodium current kinetics which are once again determined totally by the shape of the curve in Fig. 1 d and the kinetics of the change of q brought about by the particular pulse. The point is simply that because the N-system is fast all the measurable time dependent behaviour of $P(n=1)$ resides in the time dependence of the change in q.

The more detailed comparison of the model predictions with experiment given before for the squid axon (Edmonds 1987) and that given here for the frog node treated with BTX is further evidence of the applicability of silent gate models.

References

Adrian RH (1978) Charge movement in the membrane of striated muscle. Annu Rev Physiol Bioeng 7:85–112

Bergman C, Meves H (1981) The excitable membrane of nerve fibres. In: Balian R, Chabre M, Devaux PF (eds) Membranes and intercellular communication. North Holland, Amsterdam, pp 485–552

Cole K, Moore JW (1960) Potassium ion current in the squid giant axon: dynamic characteristic. Biophys J 1:1–14

Dodge FA, Frankenhauser B (1959) Sodium current in the myelinated nerve fibre of Xenopus laevis investigated with the voltage clamp technique. J Gen Physiol 148:188–200

Dubois JM, Schneider MF (1982) Kinetics of intramembrane charge movement and sodium current in frog node of Ranvier. J Gen Physiol 79:571–602

Dubois JM, Schneider MF (1985) Kinetics of intramembrane charge movement and conductance activation of Batrachotoxin-modified sodium channels in frog node of Ranvier. J Gen Physiol 86:381–394

Dubois JM, Schneider MF, Khodorov BI (1983) Voltage dependence of intramembrane charge movement and conductance activation of Batrachotoxin-modified sodium channels in frog node of Ranvier. J Gen Physiol 81: 829–844

Edmonds DT (1983) A model of sodium channel inactivation based upon the modulated blocker. Proc R Soc London Ser B219:423–438

Edmonds DT (1985) The alpha-helix dipole in membranes: a new gating mechanism for ion channels. Eur Biophys J 13:31–35

Edmonds DT (1987) A physical model of sodium channel gating. Eur Biophys J 14:195–201

Greef NG, Keynes RD, Van Helden DF (1982) Fractionation of the asymmetry current in the squid giant axon into inactivating and non-inactivating components. Proc R Soc London Ser B215:375–389

Hodgkin AL, Huxley AF (1952) A quantitative description of membrane current and its application to conduction and excitation in nerve. J Physiol 117:500–544

Keynes RD (1983) Voltage-gated ion channels in the nerve membrane. Proc R Soc Ser B220:1–30

Keynes RD, Kimura JE (1983) Kinetics of the sodium conductance in the squid giant axon. J Physiol 336:621–634

Khodorov BI (1979) Inactivation of the sodium gating current. Neuroscience 4:865–876

Meves H, Rubly N (1986) Kinetics of sodium current and gating current in the frog node of Ranvier. Pflügers Arch 407:18–26

Peganov E (1979) A study of the inactivating component of the asymmetrical current in the frog nerve fibre. Neuroscience 4:539–547

Stimers JR, Bezanilla F, Taylor RE (1985) Sodium channel activation in the squid giant axon. J Gen Physiol 85: 65–82